Relativistic effects in physics and chemistry of element 105. III. Electronic structure of hahnium oxyhalides as analogs of group 5 elements oxyhalides

V. Pershina,[a] W.-D. Sepp, T. Bastug, and B. Fricke
Theoretical Physics Department, University of Kassel, 3500 Kassel, Germany

G. V. Ionova
Institute of Physical Chemistry, Russian Academy of Sciences, Moscow Leninski pr. 31, 117915 Moscow

(Received 30 January 1992; accepted 8 April 1992)

Electronic structures of $MOCl_3$ and $MOBr_3$ molecules, where M=V, Nb, Ta, Pa, and element 105, hahnium, have been calculated using the relativistic Dirac–Slater discrete-variational method. The character of bonding has been analyzed using the Mulliken population analysis of the molecular orbitals. It was shown that hahnium oxytrihalides have similar properties to oxytrihalides of Nb and Ta and that hahnium has the highest tendency to form double bond with oxygen. Some peculiarities in the electronic structure of $HaOCl_3$ and $HaOBr_3$ result from relativistic effects. Volatilities of the oxytrihalides in comparison with the corresponding pentahalides were considered using results of the present calculations. Higher ionic character and lower covalency as well as the presence of dipole moments in MOX_3 (X=Cl, Br) molecules compared to analogous MX_5 ones are the factors contributing to their lower volatilities.

I. INTRODUCTION

In the previous work[1] we have considered electronic structure and some properties of group 5 elements pentahalides. A special attention has been given to the volatility of the pentabromides, which is a subject of intensive experimental investigations.[2]

In macrochemistry formation of the pure pentahalides, however, is often accompanied by formation of oxyhalides. If in the case of group 4 halides it is hard to suppose the formation of $MOCl_2$ molecules when MCl_4 are formed, the group 5 elements are known to form easily volatile MOX_3 (X=Cl, Br) species. Thus $NbOCl_3$ is formed during many methods directed at the preparation of niobium pentachloride and owing to their similar volatilities they are difficult to separate (ΔH_{subl} of $NbCl_5$ and $NbOCl_3$ are equal to 21.27 and 26.2 kcal/mol, respectively[3]). In the presence of even traces of oxygen at 150–200 °C pure pentahalides transform into oxytrihalide forms. Formation enthalpies of oxytrihalides in the solid state and in the gas phase are higher than those of pure halides. Thus ΔH_{form} in the solid state for $NbCl_5$ and $NbOCl_3$ are 190.2 and 210.5 kcal/mol,[3,4] respectively, and for the gas phase they were calculated from the Born–Haber cycle as 168.9 and 184.3 kcal/mol, respectively. (Data on the fluorides and oxyfluorides[5] nevertheless show that the former ones are more stable.) Thus the ΔH_{form} for TaF_5 and $TaOF_3$ are equal to 437.7 and 337.0 kcal/mol, respectively). $MOBr_3$'s are less investigated than their oxychloride analogs.

In this paper we present results of calculations of the electronic structure of the oxytrichlorides and oxytribromides of V, Nb, Ta, Pa, and of element 105, Ha, with the aim to find an analogy in their properties and, particular, in their volatilities.

In Sec. II, results of the previous experimental and theoretical investigations of the MOX_3 (M=Cl, Br) species are mentioned. Section III contains a short description of the details of the calculations in the framework of the Dirac–Slater discrete variational method (DS DVM) with self-consistent-charge (SCC) approximation. In Sec. IV results of the present molecular orbital (MO) calculations are presented. Section V is devoted to discussions of volatility of MX_5 and MOX_3 (X=Cl, Br) compounds. Conclusions are presented in Sec. VI.

II. PREVIOUS INVESTIGATIONS OF THE MOX_3 (M=V, Nb, Ta, Pa; X=Cl, Br) COMPOUNDS

A. Investigations of geometrical configurations

Of the oxyhalides MOX_3 niobium oxytrichloride is the most extensively studied. The investigations using the single-crystal x-ray diffraction technique have shown that the crystal consists of dimeric Nb_2Cl_6 units joined by niobium–oxygen linkages, so that each niobium atom has approximately octahedral coordination.[4] The infrared spectrum confirmed the existence of bridging oxygen atoms (with a strong band at 767 cm^{-1}). Data on infrared spectroscopy show that solid $NbOBr_3$ contains bridging oxygen atoms like $NbOCl_3$. Oxytribromides are only known to follow trends noted with Nb and Ta oxytrichlorides with $TaOBr_3$ being much less thermally stable and disproportioning than its niobium analog.

There are very few structural gas phase data for the oxytrihalides under consideration. Electron diffraction data[6] on $VOCl_3$ confirm that the compound is monomeric with C_{3v} symmetry, the V–Cl and V–O bond lengths being 2.12 and 1.56 Å, respectively, and the ClVCl angles being

[a]Permanent address: 117915 Moscow, Leninski pr. 31, Institute of Physical Chemistry, Russian Academy of Sciences.

 0021-9606/92/141123-09$006.00

111°. The gas-phase Raman spectrum[7] of $NbOCl_3$ has shown similarity between $VOCl_3$ and $NbOCl_3$ with niobium–oxygen vibration at 997 cm^{-1} (ν_2), which was attributed to Nb=O double bond in analogy with V=O bond (ν_2 = 1035 cm^{-1}). On the basis of this evidence it was assumed that in the gaseous state $NbOCl_3$ exists as a monomeric molecule possessing pyramidal C_{3v} symmetry.

Elements at the beginning of the actinide series have a tendency to form particularly stable MO_2^{n+} cations. Nevertheless, actinides form as well a variety of complexes with one metal–oxygen double bond as in complexes like $[MOCl_5]^{2-}$ (M=Pa, U, Np). Oxyhalides of general formula $MOCl_n$ in the solid state have oxygen atoms usually forming bridges. Protactinium, chemistry which sometimes resembles the chemistry of group 5 *d* elements, forms nonvolatile oxytrihalides. Existence of $PaOCl_3$ has not yet been confirmed, but $PaOBr_3$ is well investigated. $PaOBr_3$ crystallizes with a structure which comprises chains of seven coordinated Pa atoms linked by bridging oxygen atom and bridging bromine atom: R(Pa–O)=2.06–2.25 Å, R(Pa–Br_{br})=2.76–3.02 Å, R(Pa–Br_t)=2.56–2.69 Å (Ref. 8).

Pa–O stretching vibrations are observed only below 600 cm^{-1} which confirm the existence of bridging oxygen atoms. Oxyhalides of Pa are thermally unstable, but formation enthalpies can be only guessed by analogy with known values for $UOCl_3$ and $UOBr_3$ equal to 284.2 and 236.0 kcal/mol, respectively.[8]

B. Investigations of the electronic structures

The ability of metals to form oxycations MO^{n+} and complexes containing these cations with multiple metal–oxygen bond is a remarkable feature of the elements at the beginning of the transition series. The electronic structure of the halogen complexes of these oxycations have been the subject of both experimental and theoretical[9,10] studies. Investigations were mainly devoted to the d^1 transition metal oxohalo complexes[10] and interpretations of the extreme stability of VO^{2+} and complexes containing it. It was shown that the vanadium atom forms 1σ and 2π bonds with oxygen owing to overlap of a hybrid $3d_z^2$ orbital and $3d_{xz}$, $3d_{yz}$ ones with $2p$-oxygen orbitals, respectively. Molecular orbital calculations[10] using the multiple-scattering X_α method of the series of the d^1 complexes with V, Nb, Cr, Mo, W have shown that all these complexes have basically similar electronic structures with one MO (of a_1 symmetry) responsible for σ bonding and two MO's (of e symmetry)—for π bonding with oxygen. This multiple bonding is much stronger than single bonding metal–halogen. The reason is that two $2p_\pi$ orbitals of one oxygen atom can satisfy the π-bonding capacities of the two $3d_\pi$ orbitals of a transition metal. Is was also shown that the strength of the metal–oxygen π bonding is sensitive to the nature of the ligand atoms.

TABLE I. Input geometrical parameters: bond distances (Å), and O–M–L angles for $MOCl_3$ and $MOBr_3$.

Distance	*V*	Nb	Ta	Ha	Ha[a]	Pa[b]
a) M=O	1.56	1.66	1.67	1.74	1.72	1.74
M–Cl	2.12	2.24	2.25	2.33	2.30	2.52
b) M=O	1.56	1.70	1.71	1.79	1.75	1.74
M–Cl	2.12	2.24	2.25	2.33	2.30	2.52
c) M=O	1.56	1.70	1.71	1.79	1.75	1.74
M–Cl	2.12	2.28	2.29	2.37	2.34	2.52
∠OMCl	108°	109°	110°	111°	111°	111°
a) M=O	1.58	1.68	1.69	1.77	1.74	1.76
M–Br	2.18	2.50	2.51	2.59	2.56	2.65
∠OMBr	109°	110°	111°	112°	112°	112°

[a]Distances with relativistic bond contraction.
[b]Bond lengths for $PaOCl_3$ and $PaOBr_3$ have not been varying.

III. METHOD AND COMPUTATIONAL DETAILS OF THE MOLECULAR CALCULATIONS

A. SCC-DS DV method

The fully relativistic Dirac–Slater discrete variational method (DS DVM) with self-consistent charge (SCC) approximation developed by Rosen and Ellis[11] has been used for the present calculations. Description of the method is given in Ref. 1. The calculations have been done both within the all-electron and the frozen core approximations and for the extended basis set including valence $np_{1/2}$ and $np_{3/2}$ orbitals. Results on the charge density distribution presented in the paper are for the neutral basis set. The results obtained using the ionized basis set show the same trends for the series of molecules under consideration. Numerical integration was done using 9000 integration points.

Analysis of the charge density distribution has been done using the Mulliken breakdown scheme (see Ref. 1).

B. Input geometrical parameters

The geometry of $MOCl_3$ and $MOBr_3$ (M=Nb, Ta, Ha, and Pa) by analogy with $VOCl_3$ and $NbOCl_3$ was assumed to be C_{3v}. The molecules have a trigonal pyramid form with central atom above the equatorial plane and an oxygen atom above the metal. Experimental bond distances[3] and angles were used for $VOCl_3$ while for other molecules they were estimated based on the solid state structural data[3,4] and differences in ionic (covalent) radii.[12] Because we are not able to calculate optimal geometries we have been varying interatomic distances in quite a wide range. The influence of the specific geometry on the electronic structure will be shown in Sec. IV.

The most characteristic bond distances and angles used in the calculations are listed in Table I. The first set (a) are the shorter bond distances which were evaluated from the differences in ionic (covalent) radii[12] for V, Nb, Ta, Pa, and for Ha from the multiconfiguration Dirac–Fock (MCDF) calculations.[13] Values (Ha[a]) for $HaOCl_3$ were assumed taking into account the relativistic bond contraction (see Ref. 1). The second set (b) are bond distances where Nb=O bond length was taken from solid state data[14] for $[NbOCl_4]^-$. The third set (c) of parameters is

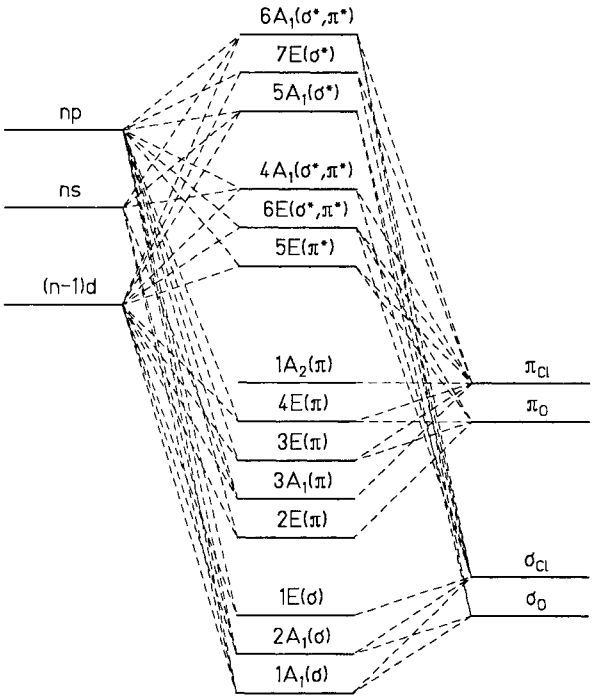

FIG. 1. Simplified MO scheme in the nonrelativistic limit for $MOCl_3$.

for the M–Cl distances taken as in the corresponding pentahalides. The geometric parameters for $MOBr_3$ (a) were estimated using the set (a) for $MOCl_3$ taking into account differences in ionic radii of Cl and Br.

IV. RESULTS AND DISCUSSION

A. Relativistic molecular orbital splitting

In the nonrelativistic limit in the C_{3v} symmetry group the *d*, *s*, and *p* valent orbitals are transformed according to irreducible representations A_1 and E. The principal scheme of molecular orbital formation for $MOCl_3$ in the nonrelativistic limit is shown in Fig. 1. In the relativistic limit for the double point group C_{3v} including time-reversal invariance, the A_1 and E representations split into the double degenerate by spin D_4 representation and nondegenerate by spin D_5 and D_6 representations. Representation A_1 is transformed into the D_4 relativistic one. Representation A_2 which in the nonrelativistic limit is a linear combination of p_π orbitals of ligands a pure nonbonding ligand orbital is transformed into D_4 relativistic representation. Double orbital degenerate representation E is split into D_4, D_5, and D_6 relativistic representations.

In Ref. 15 interpretation of the charge-transfer transitions on the basis of the nonrelativistic MO presentation has been done for $VOCl_3$. In the present calculations the $VOCl_3$ was used as a test molecule. Results obtained along with the experimental data are presented in Table II. There is quite a good agreement between the calculated and experimental values with a fine structure of lines in the spectrum (of 161 cm^{-1}) being shown by the calculations as a consequence of relativistic energy level splitting.

TABLE II. Charge-transfer electronic transitions for $VOCl_3$.

Transition	Energy, cm^{-1}	Reference
$(1a_2^2) \rightarrow (1a_2)(5e)$	29 000	Experiment (Ref. 15)
$(1a_2^2) \rightarrow (1a_2)(6e)$	40 400	
$(12D_6) \rightarrow (13D_5,D_6)$	29 276	Present
$(12D_6) \rightarrow (30D_4)$	29 437	calculations
$(12D_6) \rightarrow (31D_4)$	40 406	
$(12D_6) \rightarrow (14D_5,D_6)$	40 567	

B. Check of sensitivity of electron density distribution to changes in geometry

Since calculations of the optimal geometry is not possible due to insufficient accuracy of the numerical integration scheme, calculations of the electronic structure of $NbOCl_3$ have been done for a variety of interatomic metal–ligand distances, given in Table I, to trace the influence of this parameter on the electronic structure data. The resulting effective atomic charges, total and partial overlap populations as a function of the bond length for $NbOCl_3$ are shown in Table III.

Data in Table III show that the value of the effective charge on the metal atom is not very sensitive to the changes in the bond lengths. Thus an increase in M–Cl separation from 2.24–2.28 Å and in the M=O bond length from 1.66–1.70 Å results in a decrease in Q by only 0.02. The summary effect of the increases in both M=O and M–Cl distances by 0.10 leads to a decrease in Q of 0.05. The overlap population parameter is more sensitive to changes in the bond lengths. An increase in metal–oxygen bond length of 0.10 results in an increase in overlap population of 0.10 and an increase in the M–Cl distance brings an increase in overlap between these atoms of 0.13.

For comparison, the $NbCl_5$ molecule is also included in Table III.

TABLE III. Influence of interatomic bond distances on the charge density distribution data: effective charge (Q), total overlap population (n), and partial overlap populations ($n_{M=O}$ and n_{M-Cl}) for $NbOCl_3$ as an example.

Distance set	R(M=O), Å R(M–Cl), Å	Q	n	$n_{M=O}$ n_{M-xCl}[a]
a)	1.66	0.99	1.70	0.59
	2.24			1.11
b)	1.70	0.98	1.76	0.63
	2.24			1.13
c)	1.70	0.97	1.82	0.62
	2.28			1.19
d)	1.72	0.95	1.89	0.63
	2.33			1.26
$NbCl_5$	(ax)2.34	0.93	2.04	2.04
	(eq)2.24			

[a] $x=3$ for $NbOCL_3$; $x=5$ for $NbCl_5$.

Considering sets of the interatomic distances (a) and (b) from Table I as the most realistic ones, analysis of the electronic structure of MOX_3 molecules will be done mainly for the sets (a), because our interest is rather in the tendencies in properties of the group 5 elements than in their absolute values.

C. Molecular eigenvalues and MO composition

For the interatomic distances mentioned above [Table I, set (a)] the energy level structure as a result of the calculations for $VOCl_3$, $NbOCl_3$, $TaOCl_3$, and $HaOCl_3$ is shown in Fig. 2(a)–2(b). Molecular orbital eigenvalues are given in Table IV. Bond orders and molecular orbital compositions for these molecules are given elsewhere.[16] The ordering of energy levels is similar for $NbOCl_3$, $TaOCl_3$, and $HaOCl_3$ and valence orbital splitting in the C_{3v} symmetry group is preserved for all the molecules. The set of bonding MO's in each compound ends with MO's of $3p$(Cl) type with admixture of the oxygen changing from 21% for $NbOCl_3$ to 30% for $HaOCl_3$ [see Ref. 16 and Fig. 2(b)]. In contrast to the nonrelativistic case, where the highest occupied MO (HOMO) has pure 100% $3p_\pi$(Cl) character by symmetry, in the relativistic limit this orbital is a mixed chlorine–oxygen one. Separated from the occupied orbitals by the energy gap ΔE are MO's of predominantly d character with crystal-field splitting of d orbitals increasing from V to Ha oxychloride.

Nearly all the occupied MO's of ligand type are mixed chlorine–oxygen except one orbital: $34D_4$, $45D_4$, and $55D_4$ in $NbOCl_3$, $TaOCl_3$, and $HaOCl_3$, respectively. Energetically below these MO's are levels responsible for the metal–chlorine bonding and further down are MO's responsible for the metal–oxygen interaction. In $NbOCl_3$ these are $28D_4$, $12D_5$, $12D_6$, and $29D_4$ MO's. The $12D_5$, $12D_6$ MO's are π orbitals with high contributions (40%) of $2p_{3/2}$ orbital of oxygen and (28%) of niobium $4d_{5/2}$ orbital. Orbital $29D_4$ is of σ type and $28D_4$ is of σ and of π type. In $TaOCl_3$ orbitals responsible for metal–oxygen bonding are $39D_4$–$17D_6$ MO's and $42D_4$ MO, which is above the metal–chlorine bonding MO's. The same holds for the case of $HaOCl_3$ where the metal–oxygen $53D_4$ MO is above the metal–chlorine bonding MO's and the other three metal–oxygen MO's are $51D_4$–$22D_6$.

Complicated involvement of $(n-1)d$ metal orbitals in bonding will be shown in Sec. IV E, when considering overlap electron population data. Valence ns metal orbitals have pronounced increase in contribution to bonding in going from Nb to Ha oxychloride (see Ref. 16). This especially influences vacant orbitals of d character with admixture of ns-AO (atomic orbital). Thus the percentage of ns(metal) orbitals in the highest antibonding D_4 MO ($38D4$ and $49D4$ MO's in $NbOCl_3$ and $TaOCl_3$, respectively) increases from 4.9 up to 41.0 from $NbOCl_3$ to $HaOCl_3$. This results in stabilization of $59D_4$ MO in $HaOCl_3$ so that its position becomes below $27D_5$ and $27D_6$ orbitals [Fig. 2(b)]. Relativistic stabilization of ns-(metal) orbitals towards Ha will influence charge-transfer transition spectra in $HaOCl_3$.

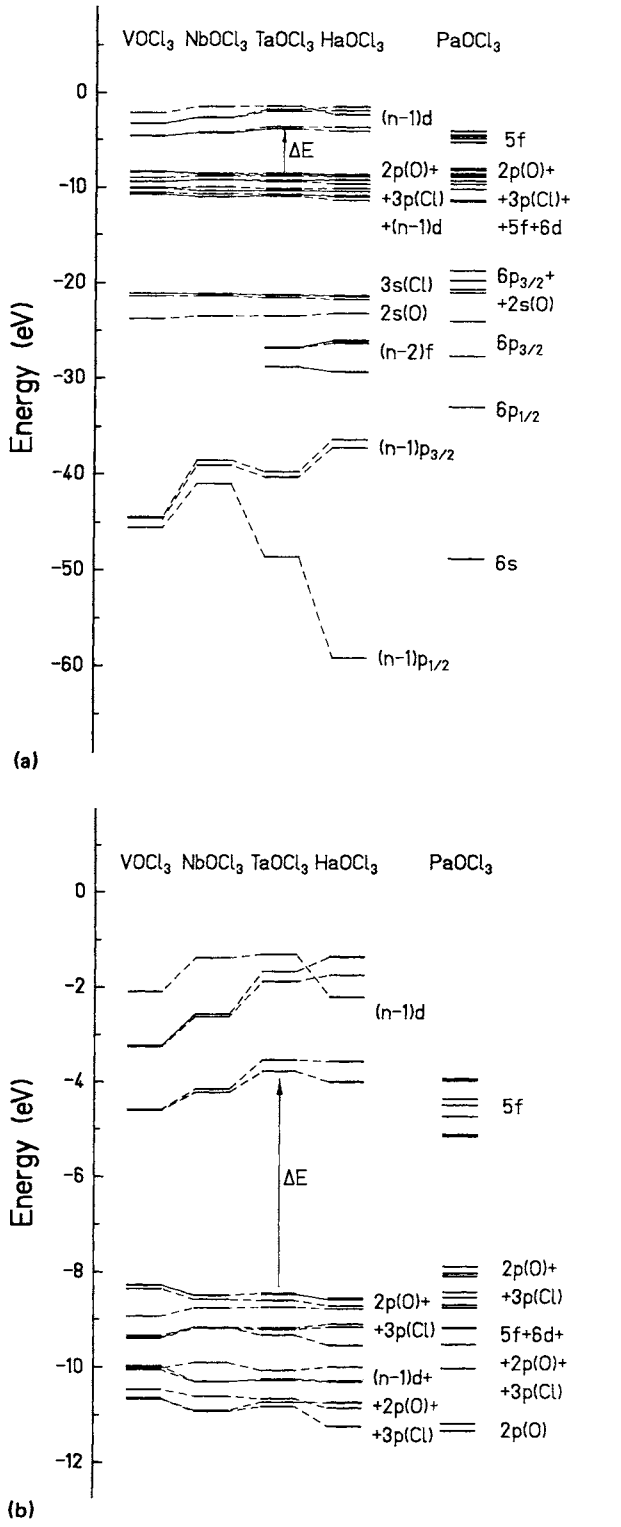

FIG. 2. (a) Energy level structure for $MOCl_3$ molecules; (b) the highest occupied and vacant levels for $MOCl_3$ molecules.

Along with the results for the d-element oxytrichlorides electronic structure, data for $PaOCl_3$ are presented in Fig. 2 and in Ref. 16. The narrow energy separation between bonding and antibonding levels and a smaller crystal field splitting of $5f$(Pa) AO's in $PaOCl_3$ is evidence of a weaker metal–ligand bonding in the f-element compound compared to the d-element ones. Chemical bonding in

TABLE IV. Molecular orbital eigenvalues for $MOCl_3$.[a]

$NbOCl_3$		$TaOCl_3$		$HaOCl_3$		$PaOCl_3$	
Orbital energy (eV)		Orbital energy (eV)		Orbital energy (eV)		Orbital energy (eV)	
...	...	...	...	...	...	25*D*5	3.93
...	...	...	...	...	...	25*D*6	3.93
38*D*4	1.38	49*D*4	1.30	27*D*6	1.35	57*D*4	3.97
17*D*6	2.55	22*D*6	1.66	27*D*5	1.36	56*D*4	4.35
17*D*5	2.56	22*D*5	1.67	60*D*4	1.75	55*D*4	4.48
37*D*4	2.61	48*D*4	1.88	59*D*4	2.20	54*D*4	4.72
36*D*4	4.15	47*D*4	3.54	58*D*4	3.57	24*D*5	5.11
16*D*6	4.21	21*D*5	3.78	26*D*6	3.99	24*D*6	5.11
16*D*5	4.22	21*D*6	3.78	26*D*5	4.00	53*D*4	5.15
15*D*6	8.48	20*D*6	8.44	25*D*6	8.54	52*D*4	7.87
35*D*4	8.49	46*D*4	8.46	57*D*4	8.57	23*D*5	8.01
15*D*5	8.49	20*D*5	8.46	25*D*5	8.57	23*D*6	8.07
34*D*4	8.57	45*D*4	8.59	56*D*4	8.70	51*D*4	8.41
33*D*4	8.75	44*D*4	8.73	55*D*4	8.76	50*D*4	8.52
14*D*5	9.15	19*D*5	9.17	24*D*5	9.09	22*D*6	8.68
32*D*4	9.16	19*D*6	9.20	24*D*6	9.15	22*D*5	8.73
14*D*6	9.18	43*D*4	9.32	54*D*4	9.53	49*D*4	8.74
31*D*4	9.90	42*D*4	10.06	53*D*4	9.99	21*D*6	9.16
13*D*5	10.29	41*D*4	10.24	52*D*4	10.28	48*D*4	9.17
13*D*6	10.29	18*D*5	10.27	23*D*6	10.29	21*D*5	9.17
30*D*4	10.30	18*D*6	10.27	23*D*5	10.30	47*D*4	9.51
29*D*4	10.61	40*D*4	10.66	22*D*6	10.73	46*D*4	10.02
12*D*6	10.89	17*D*6	10.72	22*D*5	10.74	20*D*5	11.17
12*D*5	10.90	17*D*5	10.73	51*D*4	10.85	20*D*6	11.17
28*D*4	10.92	39*D*4	10.82	50*D*4	11.23	45*D*4	11.32
11*D*5	21.12	16*D*5	21.18	21*D*5	21.22	44*D*4	18.57

[a]For the bond length [see Table I, set (a)].

$PaOCl_3$ is realized by nearly equal participation of $5f$ and $6d$ AO's of Pa (see Ref. 16). In contrast to the d-element oxytrichlorides and $PaCl_5$ (see Ref. 1), the highest occupied MO in $PaOCl_3$ has quite a pronounced contribution of the metal AO's. So $52D_4$ is not a pure ligand orbital in $PaOCl_3$ but it has 3.5% of $5f$ AO's of Pa which stabilizes this orbital and 3.9% of $6p_{3/2}$ AO which destabilizes this MO. The same situation has been observed in the uranyl compounds where the last occupied orbital has partial $5f$ character.[17] As a consequence electron transitions from the occupied orbitals to the vacant $5f$ ones are not purely charge-transfer ones but have much lower intensity and are called uranyl-like transitions. The $21D_5$–$22D_6$ orbitals in $PaOCl_3$ are responsible for the metal–chlorine bonding. Below them are orbitals of the metal–oxygen bonding character ($45D_4$–$46D_4$). Energetic stabilization of the $5f$ orbitals and their spatial contraction make metal–ligand bonding weaker compared to the d element compounds.

D. Analysis of the atomic populations

Effective atomic charges and populations of the valence atomic orbitals for the series of the molecules under consideration are presented in Tables V and VI. As in the pentahalides[1] of Nb, Ta, and Ha there is a slight increase in effective charges from Nb to Ta and there is a decrease in Q from Ta to Ha oxyhalide. Valence orbital occupancies in the nonrelativistic terms change smoothly from Nb to Ta and to Ha but in the opposite directions: $q_s = q_{s_{1/2}}$ and $q_p = q_{p_{1/2}} + q_{p_{3/2}}$ increase and $q_d = q_{d_{3/2}} + q_{d_{5/2}}$ decreases. This opposite behavior of valence AO's is the reason for nearly equal effective charges on Nb and Ta, while the general tendency in the group is an obvious decrease in ionicity. From Table V one can also see that changes in bond lengths in $MOCl_3$ do not influence much the charge–density distribution data so that basic tendencies within the group can be observed without knowing optimal geometries.

Within group 5 trends in the electronic characteristics are similar both for the oxychlorides and the oxybromides with the latter compounds being less ionic. Taking into account this fact, analysis of the electronic structure will be mainly done for the $MOCl_3$ species.

If in the nonrelativistic limit the occupancies of the valence AO's show a smooth trend from Nb to Ta and to Ha compound, relativistic orbital populations have some extremes in going from Nb to Ha oxyhalides (Tables VI). There is relative stabilization of $6p_{3/2}$ AO in $TaOCl_3(TaOBr_3)$ and relative stabilization of $d_{3/2}$ AO in $HaOCl_3(HaOBr_3)$. The general tendencies in the relativistic orbital behavior along the series of the oxytrihalides are the same as in the pentahalides considered in Ref. 1.

E. Analysis of the orbital overlap and bonding

This unsmooth change in the valence orbital involvement in bonding in going from Nb to Ta and to Ha compounds results in different overlaps of these orbitals with

TABLE V. Relativistic atomic orbital populations (q_j), overlap populations (n), effective atomic charges (Q), and dipole moments (μ) for $MOCl_3$.

AO	$VOCl_3$	$NbOCl_3$	$TaOCl_3$	$HaOCl_3$		$PaOCl_3$[a]
R(M=O), Å	1.56	1.66	1.67	1.74	1.72	1.74
R(M-Cl), Å	2.12	2.24	2.25	2.33	2.30	2.52
$q_{ns_{1/2}}$	0.19	0.18	0.29	0.48	0.47	0.16
$q_{np_{1/2}}$	0.12	0.08	0.14	0.21	0.21	0.08
$q_{np_{3/2}}$	0.23	0.14	0.18	0.12	0.12	0.07
$q_{(n-1)d_{3/2}}$	1.35	1.55	1.44	1.52	1.53	0.83
$q_{(n-1)d_{5/2}}$	1.95	2.08	1.94	1.79	1.80	1.06
n(M=O)	0.59	0.63	0.72	0.79	0.78	0.42
n(M-3Cl)	1.21	1.13	1.44	1.50	1.46	1.19
n(tot)	1.80	1.76	2.16	2.29	2.24	1.62
Q_M	1.17	0.98	1.02	0.89	0.90	1.14
Q_O	−0.40	−0.37	−0.40	−0.40	−0.40	−0.39
Q_{Cl}	−0.26	−0.20	−0.21	−0.17	−0.17	−0.25
μ, D	0.48	0.91	0.99	1.27	1.27	0.88

[a]For $PaOCl_3$: $q(5f_{5/2}) = 0.83$; $q(5f_{7/2}) = 0.93$.

the ligand orbitals and to peculiarities in the energetic characteristics (Fig. 2). Interaction of the relativistic valence orbitals with all valence AO's of oxygen and chlorine for $MOCl_3$ are shown in Table VII. The overlap of nearly all metal AO's with the ligand orbitals increases from $NbOCl_3$ to $HaOCl_3$ with the exception of $np_{3/2}$ AO, where $np_{3/2}$ orbital is destabilized not gradually from Nb to Ta and further to Ha. This results in the peak on $TaOCl_3$ and the overlap $np_{3/2}$(metal)–ligand for $HaOCl_3$ being even less than that for $NbOCl_3$.

From Table VII one can see that *ns* AO's give small overlap with oxygen even smaller than that made by *np* AO's. The biggest contribution to the metal–oxygen bonding is made by $(n-1)d$ AO's of the metals so that the amount of the electron density for $d_{3/2}$(metal)=O or $d_{5/2}$(metal)=O bonding is nearly double that for one $d_{3/2}$(metal)–Cl or $d_{5/2}$(metal)–Cl overlap. Thus Table VII shows that the double metal–oxygen bonding is made by the *nd* metal orbitals. Overlap $np_{1/2}$(metal)–oxygen or $np_{3/2}$(metal)–oxygen is of the order of one overlap np(metal)–chlorine. Hahnium forms the strongest bond with oxygen mainly due to the highest in comparison with $NbOCl_3$, $TaOCl_3$, and $PaOCl_3$ $7s_{1/2}$(metal)–oxygen and $7p_{1/2}$(metal)–oxygen overlaps as a result of the relativistic stabilization of these orbitals.

The summary data on the metal–ligand overlap for $MOCl_3$ molecules are presented in the lower part of Table V. One can see that the M=O bonding increases in going from $VOCl_3$ to $HaOCl_3$ and the general trend is the increase in the overlap population and decrease in ionicity. Tantalum oxytrichloride having nearly the same ionicity as $NbOCl_3$ nevertheless has much higher covalent binding

TABLE VI. Relativistic atomic orbital populations (q_j), overlap populations (n), and effective atomic charges (Q) for $MOBr_3$.

Molecule	$NbOBr_3$	$TaOBr_3$	$HaOBr_3$	$PaOBr_3$
R(M=O), Å	1.68	1.69	1.74	1.76
R(M-Br), Å	2.50	2.51	2.59	2.65
$q_{ns_{1/2}}$	0.26	0.46	0.63	0.18
$q_{np_{1/2}}$	0.10	0.17	0.25	0.09
$q_{np_{3/2}}$	0.18	0.21	0.15	0.08
$q_{(n-1)d_{3/2}}$	1.55	1.51	1.55	0.90
$q_{(n-1)d_{5/2}}$	2.12	1.85	1.75	1.14
n(M=O)	0.63	0.77	0.79	0.53
n(M-3Br)	1.38	1.65	1.68	1.33
n(tot)	2.00	2.42	2.47	1.86
Q_M	0.80	0.82	0.70	0.97
Q_O	−0.35	−0.37	−0.37	−0.39
Q_{Br}	−0.15	−0.15	−0.11	−0.20

TABLE VII. Partial overlap populations of the valence metal orbitals with ligand orbitals for $MOCl_3$.[a]

n	$NbOCl_3$	$TaOCl_3$	$HaOCl_3$	$PaOCl_3$[b]
$s_{1/2}$–O	0.03	0.04	0.06	0.04
$s_{1/2}$–3Cl	0.18	0.29	0.36	0.14
$s_{1/2}$(tot)	0.21	0.34	0.42	0.18
$d_{3/2}$=O	0.34	0.35	0.35	0.25
$d_{3/2}$–3Cl	0.47	0.48	0.47	0.48
$d_{3/2}$(tot)	0.81	0.82	0.82	0.73
$d_{5/2}$=O	0.51	0.53	0.54	0.36
$d_{5/2}$–3Cl	0.70	0.70	0.71	0.68
$d_{5/2}$(tot)	1.21	1.23	1.25	1.04
$p_{1/2}$–O	0.04	0.06	0.08	0.03
$p_{1/2}$–3Cl	0.10	0.15	0.20	0.09
$p_{1/2}$(tot)	0.14	0.21	0.28	0.12
$p_{3/2}$–O	0.07	0.09	0.07	0.03
$p_{3/2}$–3Cl	0.18	0.21	0.13	0.09
$p_{3/2}$(tot)	0.25	0.29	0.20	0.12

[a]For the interatomic distances [see Table I(a)].
[b]For $PaOCl_3$: $n(5f_{5/2}$=O) = 0.20; $n(5f_{5/2}$–3Cl) = 0.20; $n(5f_{7/2}$=O) = 0.28; $n(5f_{7/2}$–3Cl) = 0.25.

TABLE VIII. Ionization potentials (IP), electron affinities (EA), energies of the correspondent MO's, and first charge-transfer transitions [$E(\pi \rightarrow d)$] for $MOCl_3$ (eV).

	$VOCl_3$	$NbOCl_3$		$TaOCl_3$		$HaOCl_3$		
R(M=O), Å	1.56	1.66	1.70	1.67	1.71	1.72	1.70	1.74
R(M-Cl), Å	2.12	2.24	2.24	2.25	2.25	2.30	2.33	2.33
HOMO[a]	8.26	8.48	8.42	8.44	8.36	8.46	8.54	8.45
IP	8.46	11.60	11.55	11.57	11.48	11.64	11.64	11.53
LUMO[a]	4.64	4.22	4.26	3.78	3.80	3.83	4.00	4.01
EA	2.18	0.77	0.79	0.29	0.32	0.45	0.61	0.62
ΔE	3.46	4.27	4.26	4.66	4.56	4.63	4.54	4.44
$E(\pi \rightarrow d)$	3.65	4.57	4.48	4.98	4.88	4.94	4.84	4.74

[a]HOMO—highest occupied MO, LUMO—lowest unoccupied MO.

energy due to both metal–oxygen and metal–chlorine interactions. Hahnium oxychloride has larger metal–ligand overlap than $TaOCl_3$. The little increase in covalency in $HaOCl_3$ with respect to $TaOCl_3$ is accompanied by lowering of ionicity so that the chemical bonding in $HaOCl_3$ seems to be weaker than that in $TaOCl_3$.

Protactinium oxytrichloride has multiple metal–oxygen bond as does $MOCl_3$ of the d elements but with a different character of bonding. From Table VII it is seen that d orbitals of Pa overlap to a less extent than those of the d elements. Valent $5f$ AO's of protactinium make essential contribution to the metal–oxygen bonding. Contracted $5f$ orbitals give rather substantial interaction with oxygen (at a short distance) which is nearly of the order of interaction realized by $6d$ orbitals so that the overlap population $6d$(Pa)=O=0.61 and $5f$(Pa)=O=0.48. With the chlorines the $5f$(metal) AO's interact much weaker than $6d$ AOs: overlap populations $6d$(Pa)–Cl=1.16 and $5f$(Pa)=0.45. Atomic $6p$ orbitals act in an antibonding way in $PaOCl_3$ giving negative overlap $6p$(Pa)–O=−0.42 and $6p$(Pa)Cl=−0.29. Finally both total overlap metal–oxygen in $PaOCl_3$ and overlap metal–chlorine are less than that in the d element oxychlorides (Table V) indicating the weaker chemical interaction in the f-element compounds.

The bonding for $MOBr_3$ is shown in Table VI. The trends in the series of the oxybromides are the same as in the oxychlorides with the $MOBr_3$ having higher covalency than $MOCl_3$ due to higher metal–bromine overlap than the metal–chlorine one.

F. Ionization potentials, electron affinities, and energies of electron transitions

The complicated behavior of the relativistic MO's in the compounds under consideration gives rise to peculiarities in the energetic characteristics. In Table VIII data on ionization potentials (IP), electron affinities (EA), and energies of the first electronic charge-transfer transitions calculated via the transition-state procedure are given for some interatomic distances. These data show that ionization potentials for $MOCl_3$ increase slightly in going from $VOCl_3$ to $HaOCl_3$. The electron affinity reflects the changing position of the lowest unoccupied level in the series $MOCl_3$. As one can see from Table VIII the position of this level in $MOCl_3$ (as clearly seen in case of $HaOCl_3$) depends on the interatomic distances and mainly on the metal–chlorine distance. The composition of the lowest unoccupied MO is about 32%(Cl), 3%(O), and 65%(Ha) so that changes in the metal–chlorine distances influence stabilization–destabilization of this level. Thus in determining the electron affinity knowledge of the optimal geometry is needed. From Table VIII it is seen that the shorter the metal–chlorine separation the higher in absolute value is EA and the higher the energy of the first electron charge-transfer transition. Thus with strong relativistic contraction of bond lengths in $HaOCl_3$ stability of the pentavalent hahnium toward the process of reduction increases while any increase in bond lengths decreases this stability.

It is interesting to note that in the case of the pentahalides of the group 5 elements, tendency of hahnium to higher stability in the oxidation state 5+ for short distances is more pronounced than in $HaOCl_3$ where even at rather short bond lengths the electron affinity in $HaOCl_3$ is higher than that of $TaOCl_3$.

V. VOLATILITY OF THE $MOCl_3$ AND $MOBr_3$ COMPOUNDS

There are very few data on the melting points, boiling points, and heats of sublimation for $MOCl_3$ and $MOBr_3$ compounds.[3,4] Vanadium oxytrichloride is known as a rather volatile compound boiling at 127.2 °C. Its high volatility is a result of a monomeric structure in the solid state. Niobium oxytrichloride boils at a temperature close to that of niobium pentachloride which is equal to 247.4 °C and it has a polymeric structure like other MOX_3 (M=Nb, Ta; X=Cl, Br) compounds.

Volatility as a temperature dependence of a vapor pressure on temperature has been studied only for $NbOCl_3$ and the corresponding relation has the form

$$\log P_{mm} = 13.35 - \frac{6349}{T}, \quad (225\text{–}329\ ^\circ\text{C}).$$

Graphically this dependence along with the analogous ones for $NbCl_5$ and $TaCl_5$ are shown in Fig. 3. One can see that the vapor pressure of $NbOCl_3$ is lower than that of $TaCl_5$ and $NbCl_5$. Tantalum oxytrichloride is thermally unstable and decomposes via TaO_2Cl at 300 °C.

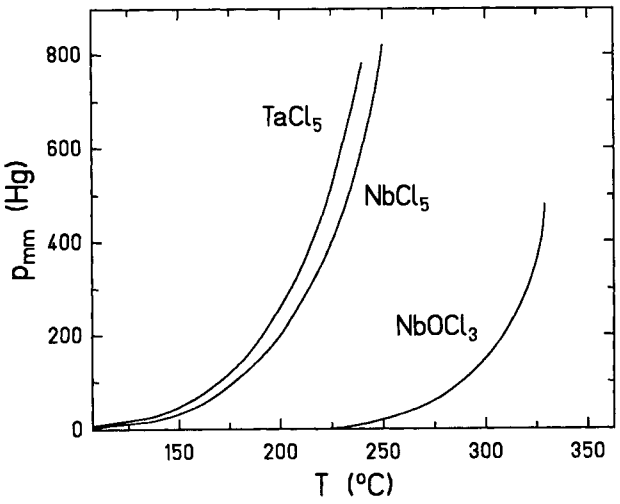

FIG. 3. Volatility as p_{mm} for $NbCl_5$, $TaCl_5$, and $NbOCl_3$ in the temperature interval 100–330 °C.

The higher boiling points of $MOCl_3$ molecules compared to the MCl_5 ones could be understood taking into account the fact that in the solid state of $MOCl_3$ the dimeric units Nb_2Cl_6 are linked via the oxygen atoms making the structure polymeric, while in the MCl_5 case the dimers Nb_2Cl_6 are independent units.

For the molecular (gas phase) state the electronic structure data, obtained as a result of the present calculations, are also indicative about lower volatility of the oxygen-containing compounds. Thus the MOX_3 molecules turn out to be more ionic than the corresponding MX_5 ones (see Tables III, V, and VI). Besides, the availability of the dipole moments in MOX_3 molecules makes an additional contribution to their higher intermolecular interaction in comparison with corresponding MX_5 ones not having dipole moments.

Consideration of the volatility of the MOX_3 species as a result of the intermolecular interaction, as it was done in our previous work,[1(b)] needs an additional information about geometry of the interaction. The interaction energy in this case will include: dipole–dipole, dipole–polarizable molecule (induction), and dispersion terms. The same holds for the interaction of MOX_3 molecules with a dielectric surface.

Among the group 5 oxyhalides the different contributions to the interaction energy may change in a different way, and even in opposite directions. Thus for element 105 depending what interaction is predominant—dispersion or dipole–dipole—the volatility may be either higher or lower than that of Nb and Ta oxyhalides, assuming that $HaOX_3$ (X=Cl, Br) in the solid state has a structure like $NbOX_3(TaOX_3)$. In case of such an opposite trend in the constituents of the interaction energy along the group the difference in volatilities between Ha and Nb(Ta) oxyhalides might be less than that between the pure pentahalides.

VI. CONCLUSIONS

Relativistic molecular orbital calculation of $MOCl_3$ and $MOBr_3$ have shown that Ha is an analog of the niobium and tantalum oxyhalides with some peculiarities in the electronic structure determined by different spin–orbital behavior within the group. In some basic properties $HaOCl_3$ follows the trends in the group: there is steady decrease in effective charges from V to Ha, increase in covalent part of the binding energy (overlap population) and increase in molecular ionization potentials.

Stability of the oxidation state 5+ should also increase down the group and for short interatomic distances (which could be realized owing to the relativistic bond contraction) $HaOCl_3$ should be nearly as stable to the process of reduction as $TaOCl_3$. For exact calculations of the electron affinity and energies of the first electron charge transfer transitions in MOX_3 the optimal geometries are needed. The chemical bonding in $HaOCl_3$ and $HaOBr_3$ seems to be weaker than that in Ta oxyhalides due to much lower ionic contribution to bonding in hahnium compounds compared to the tantalum ones.

To estimate the volatilities of $HaOX_3$ (X=Cl, Br) molecules in comparison with those for $NbOX_3$ and $TaOX_3$ ones calculations of the intermolecular interaction are needed because the possible constituents of this interaction (dispersion, dipole–dipole, dipole–polarizable molecule) can act in opposite directions. In case of such a cancelling effect the difference in volatilities between $HaOX_3$ and its analogs $NbOX_3$ and $TaOX_3$ could be less than that between HaX_5 and its analogs NbX_5 and TaX_5.

Higher ionic character and lower covalency as well as the presence of dipole moments in $MOCl_3$ molecules compared to analogous MCl_5 are factors contributing to their lower volatilities.

ACKNOWLEDGMENTS

One of us (V. Pershina) would like to thank Gesellschaft für Schwerionenforschung for financial support. We are indebted to M. Schädel, H. Gäggeler, J. Kratz, and W. Brüchle for several helpful discussions and to A. Rosen for providing us with his version of the presently used DS DVM program.

[1] (a) V. Pershina, W.-D. Sepp, B. Fricke, and A. Rosen, J. Chem. Phys. **96**, 8367 (1992); (b) V. Pershina, W.-D. Sepp, D. Kolb, B. Fricke, M. Schädel, and G. V. Ionova, *ibid.* **97**, 1116 (1992), preceding paper.
[2] H. W. Gäggeler, D. T. Jost, J. Kovacs, U. W. Scherer, A. Weber, D. Vermeulen, A. Türler, K. E. Gregorich, R. A. Henderson, K. R. Czerwinski, B. Kadkhodayan, D. M. Lee, M. J. Nurmia, D. C. Hoffman, J. V. Kratz, M. K. Gober, H. P. Zimmerman, M. Schädel, W. Brüchle, E. Schimpf, and I. Zvara, Report PSI, PSI-PR-91-32, (1991), and Radiochim. Acta (to be published).
[3] D. Brown, in *Comprehensive Inorganic Chemistry*, edited by J. C. Bailar (Pergamon, Oxford, 1973), Vol. 3, pp. 553–622.
[4] J. H. Canterford and R. Colton, *Halides of the Second and Third Row Transition Metals* (Wiley, London, 1968).
[5] K. F. Zmbov and J. L. Margrave, J. Phys. Chem. **72**, 1099 (1968).
[6] K. J. Palmer, J. Am. Chem. Soc. **60**, 2360 (1938).
[7] G. A. Ozin and D. J. Reynolds, Chem. Commun. **884** (1969).
[8] D. Brown, in *Comprehensive Inorganic Chemistry*, edited by J. C. Bailar (Pergamon, Oxford, 1973), Vol. 5, p. 187.
[9] (a) C. J. Ballhausen and H. B. Gray, Inorg. Chem. **1**, 111 (1962); (b) C. R. Hare, I. Bernal, and H. B. Gray, Inorg. Chem. **1**, 831 (1962).
[10] K. K. Sunil, J. F. Harrison, and M. T. Rogers, J. Chem. Phys. **76**, 3087 (1982).

[11] A. Rosen and D. E. Ellis, J. Chem. Phys. **62**, 3039 (1975).
[12] R. D. Shannon, Acta Crystallogr. Sect. A **32**, 751 (1976).
[13] B. Fricke and E. Johnson, Radiochim. Acta (to be published).
[14] L. G. Hubert-Pfalzgraf, M. Postel, and J. G. Riess, in *Comprehensive Coordination Chemistry*, edited by G. Wilkinson (Pergamon, Oxford, 1978), Vol. 3, p. 589.
[15] C. Dijkgraaf, Spectrochim. Acta **21**, 1419 (1965).
[16] See AIP document no. PAPS JCPSA-97-1123-8 for 8 pages of "Molecular orbitals of $NbOCl_3$, $TaOCl_3$, $HaOCl_3$, and $PaOCl_3$." Order by PAPS number and journal reference from American Institute of Physics, Physics Auxiliary Publication Service, 335 Each 45th Street, New York, NY 10017. The price is M081.50 for each microfiche (60 pages) or $5.00 for photocopies of up to 30 pages, and $0.15 for each additional page over 30 pages. Airmail additional. Make checks payable to the American Institute of Physics.
[17] J. H. Wood, M. Boring, and S. Woodruff, J. Chem. Phys. **74**, 5225 (1981).